Self-avoiding walks on Sierpinski lattices in two and three dimensions

Anke Ordemann,[1,*] Markus Porto,[2] and H. Eduardo Roman[3]
[1]*Institut für Theoretische Physik III, Justus-Liebig-Universität Giessen, Heinrich-Buff-Ring 16, 35392 Giessen, Germany*
[2]*Max-Planck-Institut für Physik komplexer Systeme, Nöthnitzer Strasse 38, 01187 Dresden, Germany*
[3]*Dipartimento di Fisica and INFN, Università di Milano, Via Celoria 16, 20133 Milano, Italy*
(Received 6 September 2001; published 17 January 2002)

The scaling properties of linear polymers on deterministic fractal structures, modeled by self-avoiding random walks (SAW) on Sierpinski lattices in two and three dimensions, are studied. To this end, all possible SAW configurations of N steps are enumerated exactly and averages over suitable sets of starting lattice points for the walks are performed to extract the mean quantities of interest reliably. We determine the critical exponent describing the mean end-to-end chemical distance $\overline{\ell}(N)$ after N steps and the corresponding distribution function, $P_S(\ell,N)$. A des Cloizeaux-type relation between the exponent characterizing the asymptotic shape of the distribution, for $\ell \to 0$ and $N \to \infty$, and the one describing the total number of SAW of N steps is suggested and supported by numerical results. These results are confronted with those obtained recently on the backbone of the incipient percolation cluster, where the corresponding exponents are very well described by a generalized des Cloizeaux relation valid for statistically self-similar structures.

DOI: 10.1103/PhysRevE.65.021107 PACS number(s): 05.40.−a, 61.41.+e, 61.43.−j

I. INTRODUCTION

The study of statistical properties of linear polymers, modeled by self-avoiding random walks (SAW) embedded in regular systems, has been extensively reported in the literature [1–3]. The effect of additional quenched disorder of the embedding matrix on the scaling behavior of SAW represents a challenging area of research, particularly for structures displaying self-similar properties where the corresponding critical exponents are expected to be different than in regular systems. Large percolation clusters at the percolation threshold are good candidates since they represent quite general models of random fractal structures (see, e.g., Refs. [4–8]). A question which is not completely understood regards the relative role of disorder and self-similarity on the distribution of the walks. To this end, the study of ordered systems such as the Sierpinski lattice, displaying exact self-similar scaling, is interesting to shed some light into this quest. This is the goal of the present paper.

The Sierpinski lattices we consider are illustrated in Fig. 1, in both $d=2$ and $d=3$ spatial dimensions. These fractal objects are characterized by a mass fractal dimension $d_S = \ln(d+1)/\ln 2$. We construct a ''large'' fractal lattice (cf. the Appendix), on which a self-avoiding walk is started at a given lattice point and is constrained to make steps between nearest-neighbor lattice sites. To study the statistical properties of the walks, we enumerate exactly all the SAW configurations of N steps. This method has proved useful in the case of disordered systems, such as the backbone of the incipient percolation cluster [6,7]. On Sierpinski lattices we study the chains using the topological metric, merely due to numerical convenience, since the chemical distance ℓ between two lattice points scales as the Euclidean distance r between them, $\ell \cong r$. A review of the present status of SAWs on Sierpinski lattices can be found in Ref. [8].

The paper is organized as follows. In Sec. II we discuss the expected scaling behaviors for the mean end-to-end chemical distance of the SAW after N steps, the scaling forms of the probability distribution function $P_S(\ell,N)$, and the total number of walks of length N, $C_{N,S}$. In Sec. III, we discuss the numerical procedure employed and report our exact enumeration results for the end-to-end distance (Sec. III A), the total number of SAW configurations (Sec. III B), and the probability distribution function (Sec. III C). Finally, Sec. IV summarizes the main results and our concluding remarks.

II. THEORETICAL RESULTS

To characterize the spatial extent of SAWs on a Sierpinski lattice let us consider the topological end-to-end distance ℓ after N steps of the walk. By averaging over all possible walks starting at a given lattice point (using exact enumeration techniques) the mean end-to-end chemical distance $\overline{\ell}(N)$ is obtained. The later is expected to scale as

$$\overline{\ell}(N) \sim N^{\nu_S}, \tag{1}$$

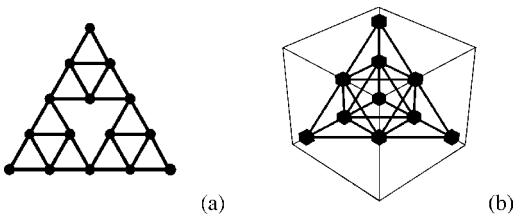

FIG. 1. Sites (circles/cubes) and bonds (thick lines) of the Sierpinski lattice in (a) $d=2$ and (b) $d=3$ dimensions, obtained after the second (a) and first generation step (b).

*Present address: Department of Physics and Astronomy, University of Missouri at St. Louis, 8001 Natural Bridge Road, St. Louis, MO 63121-4499.

which defines the critical exponent ν_S. To obtain more detailed structural information of the SAWs it is useful to determine the probability $P_S(\ell,N)d\ell$ that a walk of length N has an end-to-end distance in the range ℓ and $\ell+d\ell$. The corresponding probability distribution function (PDF) $P_S(\ell,N)$ is expected to obey the scaling form

$$P_S(\ell,N)=\frac{1}{\ell}F_S\left(\frac{\ell}{\overline{\ell}(N)}\right), \tag{2}$$

where the scaling function $F_S(x)$ is expected to behave as

$$F_S(x)=\begin{cases} x^{g_1^S+d_S} & \text{for } x\ll 1 \\ x^{g_2^S+d_S}\exp[-c_S x^{\delta_S}] & \text{for } x\gg 1, \end{cases} \tag{3}$$

and $P_S(\ell,N)$ is normalized according to $\int P_S(\ell,N)d\ell=1$.

Similarly as for SAWs on regular lattices and fractal structures, such as the incipient percolation cluster, the exponent δ_S is believed to be given by

$$\delta_S=(1-\nu_S)^{-1}, \tag{4}$$

while the remaining exponents g_1^S and g_2^S are not known so far. On regular lattices, the corresponding exponent g_1 is given by $g_1=(\gamma-1)/\nu_F$ [9], where ν_F is the Flory exponent, and the second critical exponent γ, describing the total number of SAWs of length N, is denoted as the enhancement exponent. In this work, we show that the simple generalization

$$g_1^S=\frac{\gamma_S-1}{\nu_S} \tag{5}$$

turns out to describe very well the values of g_1^S obtained numerically. This form for g_1^S should be confronted with the one recently derived in the case of SAWs on the backbone of the incipient percolation cluster, which in the Euclidean metric reads

$$g_1^r=\frac{\gamma_1-1}{\nu_r}+\frac{\beta_{\text{perc}}}{\nu_{\text{perc}}}, \tag{6}$$

denoted as the generalized des Cloizeaux relation [7]. Here, β_{perc} and ν_{perc} are the usual critical percolation exponents. The second term in Eq. (6) has its origin in the disordered nature of the backbone of percolation clusters and should not be present on deterministic fractals, such as the Sierpinski lattice. The present exact enumeration results support this conclusion.

The enhancement exponent γ_S is related to the total number of SAW configurations of length N, $C_{N,S}$, on the Sierpinski lattice by

$$C_{N,S}\sim\mu_S^N N^{\gamma_S-1}, \tag{7}$$

valid for $N\gg 1$, where μ_S is the effective coordination number of the lattice. In what follows, we discuss the numerical results and the averaging method employed.

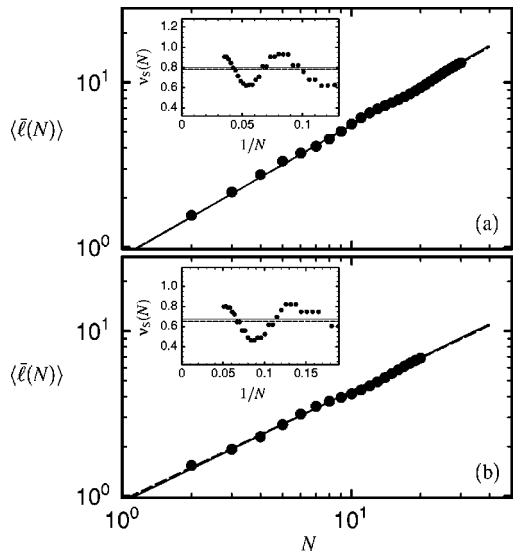

FIG. 2. Mean end-to-end chemical distance $\langle\overline{\ell}(N)\rangle$ for SAWs on the Sierpinski lattice as a function of the step length N, using exact enumeration of all walks, in (a) $d=2$ for $N\leqslant 30$, averaged over 15 starting points, and (b) $d=3$ for $N\leqslant 20$, averaged over 10 starting points. The continuous lines correspond to the values of ν_S as obtained from RG calculations [14] (cf. Table I), $\nu_S\cong 0.7986$ $(d=2)$ and $\nu_S\cong 0.67402$ $(d=3)$. The dashed lines display the present results, yielding $\nu_S\cong 0.78$ $(d=2)$ and $\nu_S\cong 0.66$ $(d=3)$. The insets display the successive slopes $\nu_S(N)\equiv d\ln\langle\overline{\ell}(N)\rangle/d\ln N$ plotted versus $1/N$.

III. NUMERICAL RESULTS

To determine the scaling exponents characterizing the probability distribution function $P_S(\ell,N)$ accurately, an average over different starting points for the SAW is required to minimize the strong lattice effects typical of the Sierpinski structure (see, e.g., [10]). Details of the method employed are discussed in the Appendix. In what follows, the average over different starting points will be indicated by the symbol $\langle\cdots\rangle$.

A. End-to-end chemical distance

The behaviors of the mean end-to-end chemical distance $\langle\overline{\ell}(N)\rangle$ as a function of step length N, obtained by exact enumeration of all walks up to $N=30$ in $d=2$ and $N=20$ in $d=3$, are displayed in Fig. 2. The insets show the effective exponents $\nu_S(N)$, obtained from the successive slopes $d\ln\langle\overline{\ell}(N)\rangle/d\ln N$, plotted as a function of $1/N$. The numerical values are reported in Table I and compared with values taken from Refs. [11–17]. The present results are in very good agreement with the known values from renormalization group (RG) calculations, in support of our approach based on the exact enumeration calculation of short chain lengths. The RG results have been obtained partly by using the fact that Sierpinski lattices belong to the same universality class as the truncated n-simplex lattices [12,18].

B. Total number of SAW configurations

To determine the enhancement exponent γ_S and the effective coordination number of the lattice μ_S, we study the

TABLE I. Numerical results for the critical exponents ν_S and γ_S, and for the effective coordination number μ_S, obtained from exact enumeration calculations of SAWs on the Sierpinski lattice in $d=2$ and $d=3$. The values reported in parentheses have been obtained by means of renormalization group techniques.

	$d=2$		$d=3$	
ν_S	0.78 ± 0.03	(0.7980[a])	0.66 ± 0.04	(0.67402[b])
γ_S	1.36 ± 0.03	(1.3752[a])	1.42 ± 0.04	(1.4461[c])
μ_S	2.29 ± 0.01	(2.28803[d])	3.82 ± 0.02	(3.815[e])

[a]References [11–14].
[b]References [15–17].
[c]Reference [11].
[d]References [12–14].
[e]Reference [12].

total number of SAWs of N steps $\langle C_{N,S}\rangle$. The expected behavior from Eq. (7) has been analyzed in two different ways, since the value of γ_S needs to be determined as precisely as possible to verify whether Eq. (5) holds. The first one consists in studying the quantity $\langle C_{N,S}\rangle\mu^{-N}$ as a function of N, for different values of μ, as shown in Fig. 3. The accepted value $\mu=\mu_S$ yields the ''best'' power-law dependence of $\langle C_{N,S}\rangle\mu^{-N}$ versus N, for large N.

The second method consists in a direct fit of the function $C_{N,S}=A_S\mu_S^N N^{\gamma_S-1}$ in the form

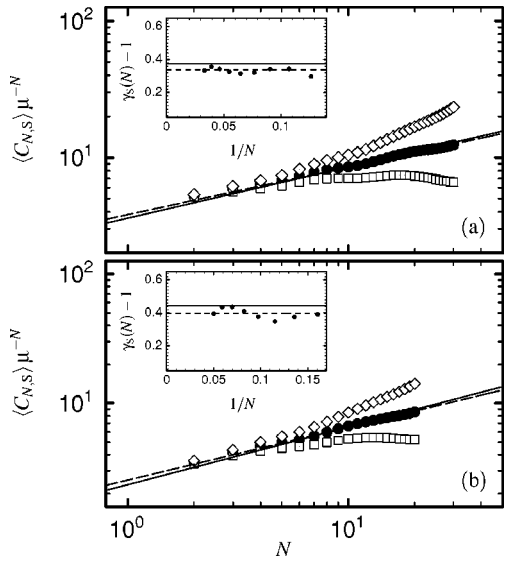

FIG. 3. Total number of SAWs of N steps $\langle C_{N,S}\rangle$ on the Sierpinski lattice: determination of the effective coordination number μ_S and enhancement exponent γ_S, by plotting $\langle C_{N,S}\rangle\mu^{-N}$ versus N in double-logarithmic form, for different values of μ. The accepted value for μ_S is obtained when $\langle C_{N,S}\rangle\mu^{-N}$ displays a satisfactory power law, and the associated slope yields γ_S-1. The plots correspond to (a) $d=2$, for $\mu=\mu_S=2.29$ (circles), $\mu=2.24$ (diamonds) and $\mu=2.34$ (squares). The dashed line is a fit yielding $\gamma_S=1.35$. It has been obtained from the successive slopes $\gamma_S(N)-1\equiv d\ln[\langle C_{N,S}\rangle\mu_S^{-N}]/d\ln N$ plotted versus $1/N$ in the inset. The continuous line in the inset represents the RG results [11–14], $\gamma_S-1\cong0.3752$. (b) $d=3$, $\mu=\mu_S=3.82$ (circles), $\mu=3.72$ (diamonds), and $\mu=3.92$ (squares). The successive slopes (inset) yield $\gamma_S=1.41$, the value is represented by the dashed line. The continuous line in the inset represents the RG results [11], $\gamma_S-1\cong0.4461$.

$$\frac{\ln\langle C_{N,S}\rangle}{N}=\frac{\ln A_S}{N}+\ln\mu_S+(\gamma_S-1)\frac{\ln N}{N} \tag{8}$$

with suitable values of the fit parameters A_S, γ_S, and μ_S. The results are shown in Fig. 4. Both methods yield consistent results and our final values are reported in Table I.

C. Probability distribution function

Our aim in studying the probability distribution for the end-to-end chemical distance for fixed number of steps N, $P_S(\ell,N)$, is to estimate the still unknown exponents g_1^S and g_2^S, in both $d=2$ and $d=3$. To minimize spurious lattice effects, we study the mean distribution $\langle P_S(\ell,N)\rangle$, averaged over different starting points, as discussed in the Appendix.

The mean PDFs are shown in Fig. 5. For $d=2$ one observes some irregularities of $\langle P_S(\ell,N)\rangle$ versus ℓ around $\ell=17$ (i.e., for $x=\ell/N^{\nu_S}\cong1.2$), whereas in $d=3$ some irregularities occur around $\ell=9$ ($x\cong1.2$) and $\ell=13$. These spurious oscillations have their origin in the structure of the underlying Sierpinski lattice, since at distances $\ell=5,9,13,17$, etc., the SAW is entering a new substructure after passing the points $\ell-1=4,8,12,16$, etc., where two substructures merge together providing a bottleneck to the SAW. If the calculations are performed by considering a single starting point for the walks, located, for instance, at a ''vertex'' of the lattice, the resulting oscillations will completely dominate

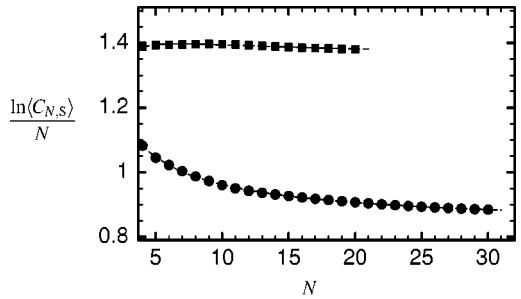

FIG. 4. Total number of SAWs of N steps $\langle C_{N,S}\rangle$, plotted as $\ln\langle C_{N,S}\rangle/N$ versus N. The lines are fits with the form $\ln\langle C_{N,S}\rangle/N=(\ln A_S)/N+\ln\mu_S+[(\gamma_S-1)\ln N]/N$ for $N\geqslant4$, in $d=2$ (circles) and $d=3$ (squares). The resulting values for the fit parameters are: $\mu_S=2.29$, $\gamma_S=1.36$, and $A_S=1.7$ in $d=2$, and $\mu_S=3.82$, $\gamma_S=1.43$, and $A_S=0.7$ in $d=3$, consistent with those obtained in Fig. 3.

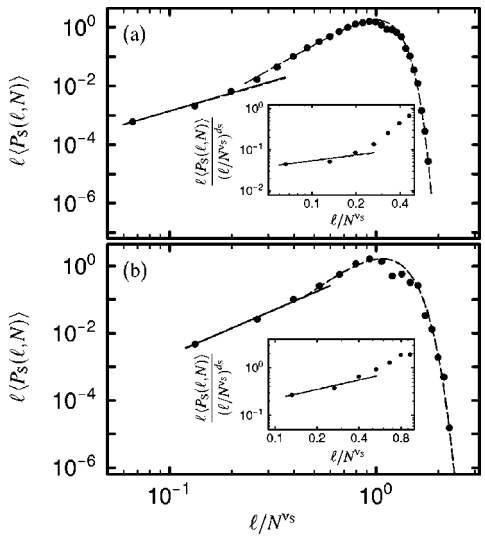

FIG. 5. Mean probability distribution function $\langle P_S(\ell,N)\rangle$ for the end-to-end chemical distance ℓ for fixed number of steps N, plotted as $\ell\langle P_S(\ell,N)\rangle$ versus ℓ/N^{ν_S}, in the cases (a) $d=2$ for $N=30$ and $\nu_S=0.78$, and (b) $d=3$ for $N=20$ and $\nu_S=0.66$. The continuous lines represent the theoretical value $g_1^S+d_S$ obtained using Eq. (5) for the RG values reported in Table I. The dashed lines in (a) and (b) represent fits of the data, in the regimes $\ell \ll N^{\nu_S}$ and $\ell \gg N^{\nu_S}$, according to Eqs. (2) and (3). The corresponding values for g_1^S are reported in Table II. (For g_2^S see Fig. 6.) A more accurate determination of the exponent g_1^S is illustrated in the insets, where the quantity $\ell\langle P_S(\ell,N)\rangle/(\ell/N^{\nu_S})^{d_S}$ is plotted versus ℓ/N^{ν_S}. The exponent g_1^S is obtained from the slope of the ansatz $\ell\langle P_S(\ell,N)\rangle/(\ell/N^{\nu_S})^{d_S}\sim(\ell/N^{\nu_S})^{g_1^S}$ for $\ell \ll N^{\nu_S}$, yielding the results: $g_1^S=0.44$ in $d=2$ and $g_1^S=0.65$ in $d=3$, in very good agreement with the theoretical prediction Eq. (5).

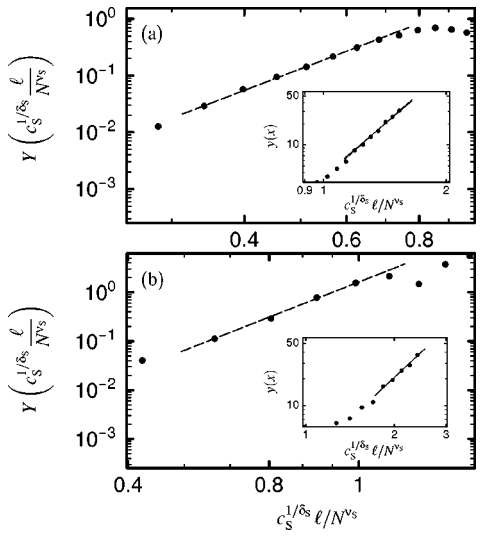

FIG. 6. Mean probability distribution function $\langle P_S(\ell,N)\rangle$ for the end-to-end chemical distance ℓ for fixed number of steps N, using the same data as in Fig. 5, for the cases (a) $d=2$ and (b) $d=3$, analyzed according to the method discussed in Ref. [6]. Self-consistent determination of g_2^S: Plotted is the quantity $Y(x)\equiv c_S^{(g_2^S+d_S)/\delta_S}(C_S')^{-1}\ell\langle P_S(\ell,N)\rangle\exp[(c_S^{1/\delta_S}\ell/N^{\nu_S})^{\delta_S}]$ versus $x\equiv c_S^{1/\delta_S}\ell/N^{\nu_S}$, with $c_S=0.47$ in $d=2$ and $c_S=1.20$ in $d=3$, which is expected to scale as $Y(x)\sim x^{g_2^S+d_S}$. Here, $\delta_S=1/(1-\nu_S)$ has been assumed, and C_S' is a constant related to the normalization of $\langle P_S(\ell,N)\rangle$. The slopes of the dashed lines represent the fitted values of $g_2^S+d_S$, which are reported in Table II. Self-consistent determination of δ_S: The insets show detailed plots to estimate the accuracy of the values of $g_2^S+d_S$ thus obtained. Plotted is the quantity $y(x)\equiv-\ln[(C_S')^{-1}c_S^{(g_2^S+d_S)/\delta_S}\ell\langle P_S(\ell,N)\rangle(c_S^{1/\delta_S}\ell/N^{\nu_S})^{-(g_2^S+d_S)}]$ versus $x\equiv c_S^{1/\delta_S}\ell/N^{\nu_S}$, expected to scale as $y(x)\sim x^{\delta_S}$, for the values of g_2^S used above. The slopes of the dashed lines represent the fit values of δ_S, in very good agreement with the values displayed by the continuous lines, obtained from Eq. (4) using the RG results for ν_S (Table I).

the PDF making it very difficult to extract the scaling exponents reliably. Although the applied averaging procedure drastically decreases the spurious oscillations, they are still apparent in Fig. 5.

The results of the fits for g_1^S, using the asymptotic scaling form Eq. (3) for $x \ll 1$, are reported in Table II. The second exponent g_2^S is determined by applying a little more sensitive approach, as illustrated in Fig. 6. The resulting values confirm those obtained from Fig. 5 and are reported in Table II. Contrary to the case of g_1^S, a theoretical estimation for g_2^S is still lacking. In d-dimensional regular systems, it is well known that g_2 is given by the relation $g_2=\delta[d(\nu_F-1/2)$

TABLE II. Critical exponents g_1^S and δ_S for SAWs on Sierpinski lattices. The first line (Theory) reports the theoretical values obtained from Eq. (5) and Eq. (4), respectively, using the values of ν_S and γ_S reported in Table I. The second line (Fit) reports numerical values obtained directly from the plots of the PDF displayed in Fig. 5 and Fig. 6. The third line (RG) reports the results from RG calculations using the RG values of ν_S and γ_S from Table I together with Eq. (5) and Eq. (4). The bottom line of the table contains the values of g_2^S obtained directly from the PDF (Fig. 6).

		$d=2$	$d=3$
g_1^S	Theory	0.46 ± 0.04	0.64 ± 0.07
	Fit (Fig. 5)	0.44 ± 0.05	0.65 ± 0.08
	RG [Eq. (5)]	0.470	0.662
δ_S	Theory	4.77 ± 0.25	2.94 ± 0.20
	Fit (Fig. 6)	5.1 ± 0.2	3.0 ± 0.3
	RG [Eq. (4)]	4.965	3.068
g_2^S	Fit (Fig. 6)	2.34 ± 0.10	2.6 ± 0.4

$-(\gamma-1)]$ [19], where $\delta=1/(1-\nu_F)$. Unfortunately, a straightforward extension of this form to the Sierpinski lattice (as well as to percolation cluster) does not lead to good results.

IV. DISCUSSION

We have studied scaling properties of SAWs on Sierpinski lattices using exact enumeration techniques of all walks up to a length N, in both $d=2$ ($N\leqslant 30$) and $d=3$ ($N\leqslant 20$) spatial dimensions. We have determined the critical exponent ν_S, describing the spatial extent of the walks, the enhancement exponent γ_S and the effective coordination number of the lattice μ_S, both describing the total number of SAW configurations of N steps.

Our numerical results are consistent with renormalization group values known in the literature. We find that γ_S in $d=3$ is larger than the value in $d=2$, in agreement with the results by Dhar [11], possibly indicating that γ_S increases by increasing the dimensionality of the Sierpinski lattice. This is also consistent with the prediction $\gamma\rightarrow 1.618$ for $d\rightarrow\infty$ obtained in Ref. [20]. Note that this behavior is opposite to that found on regular systems, for which $\gamma\approx 1+(4-d)/6$ [21] decreases and becomes equal to 1 at and above the critical dimension $d=d_c=4$ (see, e.g., [1,3]), as well as to that observed on the incipient percolation cluster, for which γ also decreases and becomes equal to 1 at and above the critical dimension $d=d_c=6$ (see, e.g., [6,7]). Our results for γ_S may be an indication of the absence of an upper critical dimension of SAWs on Sierpinski lattices.

Regarding the probability distribution function of SAWs for fixed N, $P_S(\not{\ell},N)$, we have studied its scaling forms and have determined the corresponding exponents, g_1^S and g_2^S, characterizing the associated scaling function, values which were unknown so far. We have proposed a simple theoretical form for g_1^S, i.e., $g_1^S=(\gamma_S-1)/\nu_S$, which describes very well the present numerical values.

This latter relation is interesting, since it is different from the one recently proposed for SAWs on the backbone of the incipient percolation cluster [7] [cf. Eq. (6)]. The main difference resides in the fact that the backbone is a disordered fractal, where the probability that the walk returns close to its starting point after a large number of steps N depends on additional constraints due to the statistical nature of the self-similar system. In this sense, Sierpinski lattices are more similar to regular systems than to disordered fractal structures. It would be interesting to study SAWs on other disordered as well as deterministic self-similar structures to confirm our findings.

ACKNOWLEDGMENTS

We acknowledge fruitful and stimulating discussions with S. Havlin. Financial support from the Deutsche Forschungsgemeinschaft is gratefully acknowledged.

APPENDIX: SIERPINSKI LATTICE AND AVERAGING PROCEDURE FOR THE SAWs

It is known that PDFs and other observables on deterministic fractals, such as the Sierpinski lattice, often display an undesired alternating behavior as a function of the position due to lattice effects (see, e.g., [10]). The latter introduce additional difficulties for the evaluation of the corresponding scaling exponents. To minimize such lattice effects and to allow precise estimates for the scaling exponents, we have implemented an averaging procedure in which (typically 10–15) different, and nonequivalent, lattice points are considered as starting points of the SAWs. The starting points (as well as the lattice size) are chosen such that an SAW starting in any of these points is not able to reach the lattice boundary. A mean PDF, for example, is obtained by averaging over the associated PDF corresponding to each starting point.

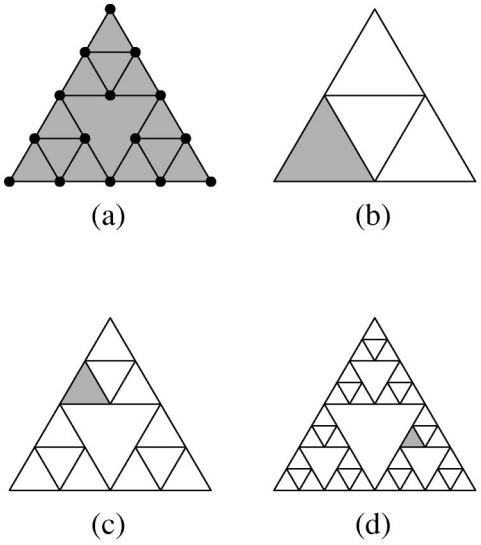

FIG. 7. Illustration of the choice of starting points for SAWs on the Sierpinski lattice in $d=2$ and the lattice construction procedure used in this work. In (a) the corresponding lattice is shown up to the second generation step, where the set of starting lattice points are indicated by the full circles. The fractal lattice is constructed in such a way that the shadowed triangle, containing the starting points, remains located as close as possible to the center of the lattice, thus eliminating lattice boundary effects for the chain lengths considered. The plots in (b), (c), and (d) illustrate the initial construction steps.

The chosen set of starting points for the two-dimensional case, constituted of 15 points and obtained at the second generation step of the fractal, is illustrated in Fig. 7. In $d=3$, the set amounts to ten points corresponding to the first generation step (cf. Fig. 1). The construction procedure is performed in such a way that the set of starting points remains located as close as possible to the center of the lattice in order to eliminate boundary effects, and the lattice is grown in a circular fashion until it is guaranteed that the SAW cannot reach the lattice boundary [cf. Figs. 7(b)–7(d)]. In our calculations, we have considered chains of $N\leqslant 30$ steps in $d=2$ and $N\leqslant 20$ steps in $d=3$. To avoid finite lattice effects we have grown a fractal lattice up the seventh generation step in $d=2$, corresponding to 3282 lattice points, and up to the sixth step in $d=3$ corresponding to 8194 lattice sites.

[1] P.-G. de Gennes, *Scaling Concepts in Polymer Physics* (Cornell University Press, Ithaca, 1979).
[2] M. Doi and S. F. Edwards, *The Theory of Polymers Dynamics* (Clarendon, Oxford, 1986).
[3] J. des Cloizeaux and G. Jannink, *Polymers in Solution: Their Modelling and Structure* (Clarendon, Oxford, 1990).
[4] K. Barat and B. K. Chakrabarti, Phys. Rep. **28**, 377 (1995).
[5] D. Ben-Avraham and S. Havlin, *Diffusion and Reactions in Fractals and Disordered Systems* (Cambridge University Press, Cambridge, 2000).
[6] A. Ordemann, M. Porto, H. E. Roman, S. Havlin, and A. Bunde, Phys. Rev. E **61**, 6858 (2000); note that on page 6860 of this publication, Ref. 36 should have been quoted in the right column below Eq. (6) instead of the erroneously cited Ref. 30, and that Ref. 30 should have appeared in the discussion of Monte Carlo simulations of SAW on percolation cluster in the lower right column of page 6861.
[7] A. Ordemann, M. Porto, H. E. Roman, and S. Havlin, Phys. Rev. E **63**, 020104(R) (2001).
[8] B. D. Hughes, *Random Walks and Random Environments* (Clarendon, Oxford, 1995).
[9] J. des Cloizeaux, Phys. Rev. A **10**, 1665 (1974).
[10] L. Acedo and S. B. Yuste, Phys. Rev. E **63**, 011105 (2000).
[11] D. Dhar, J. Math. Phys. **19**, 5 (1978).
[12] R. Rammal, G. Toulouse, and J. Vannimenus, J. Phys. (Paris) **45**, 389 (1984).
[13] D. J. Klein and W. A. Seitz, J. Phys. (France) Lett. **45**, L241 (1984).
[14] D. Kim and B. Kahng, Phys. Rev. A **31**, 1193 (1985).
[15] T. Hattori and S. Kusuoka, Probability Theory Related Fields **93**, 273 (1992).
[16] K. Hattori, T. Hattori, and S. Kusuoka, Publ. Res. Inst. Math. Sci. **29**, 455 (1993).
[17] T. Hattori and H. Nakajima, Phys. Rev. E **52**, 1202 (1995).
[18] D. Dhar, J. Math. Phys. **18**, 577 (1977).
[19] D. McKennzie and M. Moore, J. Phys. A **4**, L82 (1971).
[20] S. Kumar, Y. Singh, and Y. Joshi, J. Phys. A **23**, 2987 (1990).
[21] H. E. Roman, Phys. Rev. E **51**, 5422 (1995).